



HAL
open science

Advanced infections by cucurbit yellow stunting disorder virus encourage whitefly vector colonization while discouraging non-vector aphid competitors

Quentin Chesnais, Penglin Sun, Kerry Mauck

► To cite this version:

Quentin Chesnais, Penglin Sun, Kerry Mauck. Advanced infections by cucurbit yellow stunting disorder virus encourage whitefly vector colonization while discouraging non-vector aphid competitors. Journal of Pest Science, 2022, 95 (1), pp.231-247. 10.1007/s10340-021-01394-z . hal-03484012

HAL Id: hal-03484012

<https://hal.inrae.fr/hal-03484012v1>

Submitted on 9 Oct 2023

HAL is a multi-disciplinary open access archive for the deposit and dissemination of scientific research documents, whether they are published or not. The documents may come from teaching and research institutions in France or abroad, or from public or private research centers.

L'archive ouverte pluridisciplinaire **HAL**, est destinée au dépôt et à la diffusion de documents scientifiques de niveau recherche, publiés ou non, émanant des établissements d'enseignement et de recherche français ou étrangers, des laboratoires publics ou privés.



Distributed under a Creative Commons Attribution 4.0 International License

1 **Advanced infections by cucurbit yellow stunting disorder virus encourage whitefly vector**
2 **colonization while discouraging non-vector aphid competitors**

3

4 Quentin Chesnais^{1,2}, Penglin Sun², Kerry E. Mauck²

5

6 ¹Institut National de Recherche en Agriculture, Alimentation et Environnement, SVQV UMR-
7 A1131, Université de Strasbourg, 68000 Colmar, France.

8 ²Department of Entomology, University of California, Riverside, Riverside, CA 92521, USA

9 Corresponding Authors: Quentin Chesnais (quentin.chesnais@inrae.fr) and Kerry Mauck
10 (kerry.mauck@ucr.edu)

11

12 **Abstract**

13 Plant viruses can change hosts in ways that increase vector contacts, virion acquisition, and
14 subsequent vector dispersal to susceptible hosts. Based on this, researchers have proposed
15 that virus-induced phenotypes are the product of adaptations to “manipulate” hosts in ways
16 that increase transmission. Theoretical models of virus spread in crops support this
17 proposition; “manipulative” viruses spread faster and to a greater extent. However, both
18 empirical and theoretical studies on manipulation are disproportionately focused on a few
19 persistently transmitted pathogens, and rarely consider the broader ecological implications of
20 virus infections . To address these knowledge gaps, we documented the effects of
21 different stages of infection by an economically devastating, semi-persistently transmitted
22 crinivirus, *Cucurbit yellow stunting disorder virus* [CYSDV] on *Cucumis melo* (muskmelon)
23 phenotypes, behavior and performance of whitefly vectors (*Bemisia tabaci*) and non-vector
24 aphid competitors (*Aphis gossypii*). Whiteflies were strongly attracted to CYSDV-infected
25 hosts in a symptomatic stage of disease , but not in an asymptomatic stage, and fed more
26 easily on infected plants regardless of symptoms . In contrast, aphids tended to avoid
27 infected hosts, fed for shorter periods of time, and produced fewer offspring on infected
28 hosts . Metabolomics revealed that host manipulations by CYSDV do not rely on virus-
29 induced shifts in leaf primary metabolites or volatiles but may involve changes to phloem
30 architecture and other compounds not measured here. Our study demonstrates a
31 sophisticated host manipulation by CYSDV, whereby infection discourages colonization by a
32 non-vector competitor while inducing a suite of progressively more transmission-conducive
33 changes that encourage virion acquisition by the vector.

34

35

36 **Keywords**

37 disease progression, electrical penetration graph, plant virus manipulation, plant volatiles,
38 vector behavior, virus ecology

39

40 **Declarations**

41 **Funding** Funding for this work was provided by the California Melon Research Board, Hatch
42 project funds (CA-R-ENT-5144-H), the Specialty Crop Block Grant Program (18-0001-065-
43 sc), and the University of California, Riverside.

44

45 **Conflicts of interest/Competing interests** The authors declare that they have no conflict of
46 interest. The funders had no role in the design of the study, in the analyses, or interpretation
47 of data; in the writing of the manuscript, or in the decision to publish the results.

48

49 **Availability of data and material** UC Riverside partners with Dryad data repository. All data
50 will be made available through Dryad once a manuscript number is assigned to complete the
51 dataset submission. The manuscript number is required to link data to a manuscript in
52 progress. This data statement will be updated should the manuscript be accepted.

53

54 **Code availability** Not applicable

55

56 **Authors' Contributions** KEM and QC conceived the ideas and designed experiments; PS
57 and KEM designed methods for metabolite analysis; QC and PS collected the data; QC led
58 data analysis with input from KEM; KEM led writing of the manuscript and all authors
59 contributed critically to the drafts and gave final approval for publication.

60

61 **Ethics approval** The article does not contain any studies with human participants or
62 vertebrate animals. The authors affirm that all work was performed in accordance with state
63 and federal permit conditions for work with pest insects and pathogens of plants.

64

65 **Consent to participate** (N/A)

66

67 **Consent to publication** (N/A)

68

69 **Acknowledgements** Special thanks to William M. Wintermantel (USDA-ARS) for providing
70 CYSDV inoculum to begin our laboratory culture, Martha S. Hunter (U. of Arizona) for
71 providing *B. tabaci*, and Gregory P. Walker (UC Riverside) for providing *A. gossypii*. Insect
72 colony maintenance was provided by T. Shates, J. Kenney, and I. Wright.

73

74 **Key Message**

75

- 76 ● Plant viruses may evolve to manipulate hosts in ways that encourage transmission
- 77 by vectors.
- 78 ● Manipulation work focuses on a narrow range of viruses and excludes most
- 79 ecological contexts.
- 80 ● We studied effects of CYSDV: a virus with an understudied semi-persistent
- 81 transmission mode.
- 82 ● We evaluated host phenotypes across disease progression and vector-competitor
- 83 interactions.
- 84 ● CYSDV manipulates hosts to increase vector contacts and decrease feeding by non-
- 85 vector pests.
- 86 ● Host manipulation by CYSDV occurs through multiple routes and can be a target for
- 87 management.
- 88

89 **Introduction**

90 Virus infections often alter plant phenotypes, with significant consequences for host survival,
 91 fitness, and interactions with other organisms (Davis et al. 2015; Eigenbrode et al. 2017;
 92 Mauck et al. 2018; González et al. 2020). In the case of arthropod-transmitted plant viruses,
 93 such effects can also influence interactions with the mobile vectors. Given the importance of
 94 vector-host interactions for transmission, we might expect that selection should favor viruses
 95 that change host phenotypes in ways that increase (or at least maintain) vector contacts and
 96 feeding behaviors that facilitate virion acquisition (Mauck et al. 2016). In line with this
 97 expectation, there are now numerous published reports of viruses altering host phenotypes
 98 in ways that should enhance dissemination by vectors (Eigenbrode et al. 2017; Mauck et al.
 99 2018). The bulk of these studies document changes in vector orientation, feeding, and/or
 100 dispersal behaviors through choice and no-choice behavioral bioassays (reviewed in (Mauck
 101 et al. 2018; Mauck and Chesnais 2020)) and a small number have identified specific host
 102 metabolic changes and virus components responsible for eliciting these effects (reviewed in
 103 (Mauck et al. 2019; Ziegler-Graff 2020)). Building upon empirical work, several mathematical
 104 modeling papers suggest that “manipulative” plant viruses spread more rapidly and to a
 105 greater extent, especially in monocultures, relative to those having no effect on host-vector
 106 interactions (Roosien et al. 2013; Shaw et al. 2017). Collectively, this body of work provides
 107 mounting evidence that virus effects on host phenotypes can influence the probability of
 108 subsequent transmission by vectors, and that such effects may be the product of virus
 109 adaptations that persist because of the transmission benefits they confer.

110

111 The idea that plant viruses can be selected for “manipulating” their hosts to enhance
 112 plant-vector contacts has fueled an increasing number of studies across a growing diversity

113 of pathosystems (Mauck et al. 2018). However, these are strongly biased toward a few taxa
114 with limited diversity of transmission modes. For example, in a survey of virus effects on host
115 phenotypes, we found that viruses having a circulative, persistent transmission mode were
116 overrepresented among both empirical and theoretical studies, and that within this category,
117 the majority of studies focused on viruses from just one family - *Luteoviridae* (Mauck et al.
118 2018; Mauck and Chesnais 2020). As a result, the study area of 'virus manipulation' lacks
119 information on some of the most important emerging pathogens of concern for agriculture,
120 especially viruses with semi-persistent transmission modes and highly polyphagous vectors
121 (Tzanetakis et al. 2013; Fereres et al. 2016; Maluta et al. 2017; Maluta et al. 2019; Pereira et
122 al. 2019; Ertunc 2020). Beyond limitations on the taxonomic diversity of studied
123 pathosystems, our understanding of virus manipulations and its implications for agriculture is
124 further limited by an emphasis on overly simplified scenarios in empirical work. Even for the
125 most well-studied pathosystems, only a handful of studies, if any, have considered virus
126 manipulation of hosts and vectors in the context of disease progression, host survival, and
127 species interactions among manipulated hosts and other organisms (Mauck and Chesnais
128 2020).

129

130 These omissions limit our ability to discern if virus-induced phenotypes are robust
131 within the very environments in which manipulative virus traits are purported to have
132 evolved. Although time and disease progression are major considerations in plant virus
133 epidemiology, documented instances of putative host manipulation by plant viruses
134 overwhelmingly focus on a single time point. Arbitrary time point selection by a researcher
135 will potentially determine whether a virus-induced phenotype is concluded to be adaptive for
136 the virus (neutral or transmission-enhancing), or detrimental (transmission-limiting).
137 Likewise, virus-induced phenotypes that appear to be conducive to transmission in the
138 laboratory, but which compromise host survival in the context of additional biotic or abiotic
139 stressors, are unlikely to be favored by selection, as the longevity of a host as an inoculum
140 source for virus acquisition by vectors could be significantly reduced. If this is the case in a
141 crop host, it would mean that the phenotype induced by the virus is not likely to be a useful
142 target for management (e.g., through rogueing of infected plants that attract vectors).

143

144 In the present study, we focus on these shortcomings and begin to address them in
145 several ways. In response to the relative lack of studies on semi-persistently transmitted
146 viruses compared to viruses with other transmission modes, we decided to focus on an
147 economically important emerging virus that is a major pathogen in cucurbit agroecosystems
148 around the world: the whitefly-transmitted *Cucurbit yellow stunting disorder virus* (CYSDV)
149 (genus *Crinivirus*, family *Closteroviridae*) (Tzanetakis et al. 2013; Wintermantel et al. 2017).

150 This pathogen is presently the most serious virus threat to muskmelon (*Cucumis melo*)
151 production in the United States, particularly in the Southwest, where approximately 75% of
152 U.S. melon production takes place (Wintermantel et al. 2017). Rapid secondary spread
153 occurs from initial melon infections within a single growing season, with fields often reaching
154 100% infection by harvest date (Wintermantel et al. 2017). This suggests that host and
155 vector manipulation may play a significant role in the epidemiology of this pathogen.

156

157 To explore this while also addressing the need to consider the dynamic nature of
158 virus-induced phenotypes, we evaluated virus effects on host-vector interactions at pre-
159 symptomatic and post-symptomatic time points in disease progression in the primary crop
160 host (*Cucumis melo*). These organismal experiments were complemented by chemical
161 analysis of volatile and non-volatile plant metabolites known to play important roles in host-
162 vector interactions. CYSDV is transmitted in a semi-persistent manner by whiteflies and is
163 acquired from the phloem (Celix et al. 1996; Wintermantel et al. 2017). Therefore, we
164 hypothesized that a transmission-conducive phenotype in CYSDV-infected *C. melo* would
165 include changes that enhance whitefly attraction and facilitate increased uptake of phloem
166 sap followed by eventual dispersal after sufficient feeding to become viruliferous. In prior
167 work, we found evidence that CYSDV-induced changes in *C. melo* stimulate whitefly
168 attraction and settling at a time point where symptoms are strongly apparent (four weeks
169 post-inoculation) and that attenuation of symptoms using defense priming of the immune
170 system disrupts whitefly preferences at this time point (Kenney et al. 2020).

171

172 To place our findings in a semi-ecological context, we further combine virus-host-
173 vector studies with an exploration of how time and virus infection interact to modify the
174 susceptibility of hosts to a ubiquitous *C. melo* pest that shares the same ecological niche as
175 the whitefly vector: the cotton-melon aphid, *Aphis gossypii* (Hemiptera: Aphididae) (Capinera
176 2009). Aphids and whiteflies negatively affect hosts by direct removal of resources and
177 through secretion of effector molecules that modify the plant immune system (Kaloshian and
178 Walling 2016; Erb and Reymond 2019). Plants have counter-defenses that mitigate impacts
179 of herbivore feeding by repelling herbivores (antixenosis), reducing herbivore performance,
180 survival, or reproduction (antibiosis), or by enabling tolerance even under moderate levels of
181 herbivory (Núñez-Farfán et al. 2007; Mitchell et al. 2016). Virus infection can fundamentally
182 change the expression of these traits as a component of vector manipulation strategies. But
183 under real-world conditions, this may not always be beneficial for the virus if transmission-
184 conducive host phenotypes are also more attractive to, or more easily exploited by, non-
185 vector herbivores (Belliure et al. 2010; He et al. 2012; Nachappa et al. 2013; Kersch-Becker
186 and Thaler 2014; Su et al. 2016; Peñafior et al. 2016; Ángeles-López et al. 2017). This could

187 ultimately be detrimental for virus fitness if vectors encounter more competition on infected
188 hosts or if novel susceptibility phenotypes accelerate host decline. Non-vectors that initially
189 benefit from virus-induced changes can also modify plants over time in ways that counteract
190 virus manipulations of the same pathways (Ángeles-López et al. 2017). Thus, exploring
191 broader “off-target” effects of putative manipulations can provide insight into the adaptive
192 significance of virus effects on host phenotypes; a necessary step before proceeding with
193 mechanistic studies to identify genetic variations associated with manipulative effects
194 (Mauck et al. 2019) or studies to disrupt virus manipulation in crops (Bak et al. 2019).

195

196 Given the overlap among whiteflies and the cotton-melon aphid in cues used for host
197 selection, feeding locations, resources consumed, and defensive pathways altered (Zarate
198 et al. 2007; Rodriguez et al. 2014; Mugford et al. 2016; Xu et al. 2019; Cui et al. 2019), we
199 consider it an essential step to determine if there is also overlap in responses to putative
200 host manipulations by CYSDV. We explored these possible off-target effects in tandem with
201 on-target putative manipulations across two time points in disease progression (pre-
202 symptomatic and symptomatic) relative to sham-inoculated non-infected hosts in the same
203 phenological stages. Behavior and performance assays for both insects are considered in
204 the context of symptom expression, primary metabolites, leaf color, and odor cues. Exploring
205 the spectrum of changes that drive insect selection among CYSDV-infected and non-
206 infected hosts has revealed the extent to which CYSDV may manipulate its own
207 transmission in the field, as well as new pathways to target for disrupting vector attraction.

208

209 **Materials and methods**

210 **Organisms**

211 Whiteflies (*Bemisia tabaci* MEAM1 biotype, formerly biotype B; Hemiptera: Aleyrodidae)
212 were collected in 2006 from cotton at the Maricopa Agricultural Center, AZ, USA (Himler et
213 al. 2011). *Aphis gossypii* used in our experiments were established from aphids collected
214 from squash about a decade ago near Reedley, CA, USA. Melons (*Cucumis melo* cv.
215 “Iroquois”) served as the host in all experiments and were used to maintain the aphid colony.
216 We used cowpea plants (*Vigna unguiculata* cv. “CT Pinkeye Purple Hull”) to maintain the
217 whitefly colonies. We sowed seeds individually in starter trays, then transplanted seedlings
218 into 10*10*10 cm pots filled with UC Soil Mix 2 (Matkin and Chandler 1957) and
219 approximately 4g of Osmocote slow-release 14-14-14 fertilizer with micronutrients. Melons
220 and cowpeas were maintained in an insect-free growth chamber (23 ± 1 °C, 60 ± 5% RH,
221 and 16L:8D photoperiod) until ready for use in colonies.

222

223 The isolate of CYSDV used in experiments was originally collected from muskmelons
224 in the Imperial Valley in 2006 Bill Wintermantel (USDA-ARS, Salinas) who initiated a pure
225 culture and maintained the virus on *C. melo* (Wintermantel et al. 2009). We maintained
226 CYSDV in Iroquois melons growing in bugdorms in a climate-controlled greenhouse with
227 supplementary LED lighting (25 ± 1 °C, $60 \pm 5\%$ RH, and 16L:8D photoperiod). We
228 performed transmissions by allowing whiteflies to feed for 48-h on CYSDV-infected melon
229 plants (acquisition access period) and then by transferring 25-30 whiteflies to plants in the
230 first true leaf phenological stage (two-week-old plants) for a three-day inoculation access
231 period. We then gently removed whiteflies with an aspirator. Symptom development
232 consisting of yellowing of leaf margins and interveinal discoloration was observable after ~21
233 days post-inoculation (dpi) and virus infection was also confirmed using double-antibody
234 sandwich enzyme-linked immunosorbent assay with polyclonal CYSDV antibodies
235 (BIOREBA CYSDV complete kit 960, Art No. 162372). We treated sham-inoculated (i.e.,
236 non-infected) plants similarly using non-viruliferous whiteflies. All bioassays described below
237 were carried out on plants at two- or four-weeks post-inoculation or post sham-inoculation
238 (wpi) in a greenhouse under controlled conditions (25 ± 1 °C, $60 \pm 5\%$ RH, and 16L:8D
239 photoperiod). Comparisons of 2 wpi and 4 wpi plants (and sham controls) necessitated
240 performing inoculations of these cohorts separately (i.e., plants in the 4 wpi cohort, followed
241 2 weeks later by plants in the 2 wpi cohort). To minimize any confounding factors, 2 wpi and
242 4 wpi plants received CYSDV from the same source culture and were grown on the same
243 bench in the same greenhouse using identical culture methods.

244

245 ***Whitefly and aphid preference tests***

246 We assessed whitefly preferences through assays allowing access to all cues (volatile,
247 visual, and contact) and assays allowing only volatile cues. For the all-cue preference
248 assays, groups of 30 non-viruliferous whiteflies were allowed to select among four
249 treatments consisting of two CYSDV-infected melon plants (one 2 wpi and the other 4 wpi)
250 and two sham-inoculated melon plants (one 2 weeks post sham-inoculation and the other 4
251 weeks post sham-inoculation). Presence of a whitefly on the surface of one of these
252 treatments (settling) was considered a choice and whitefly positions among treatments were
253 evaluated at 1, 2, and 24 hours after release. Assays were conducted as in Kenney et al.
254 (2020) and are described in detail in the Electronic Supplementary Materials (ESM). We
255 performed assays permitting access to only volatile cues in an opaque arena described in
256 detail in Supplementary Figure 2. We performed 16 replications of dual choice tests between
257 4 wpi CYSDV-infected plants and their corresponding sham-inoculated plants. We chose to
258 focus on this treatment pair because CYSDV-infected plants at 4 wpi were the only
259 treatment to elicit whitefly attraction in the full-cue access tests. Whiteflies on each mesh-

260 covered hole were counted at 5, 10, 15, and 20 minutes, then averaged across all time
261 points (as in Mauck et al. 2010) and converted to percentages of the total whiteflies that had
262 entered the arena.

263 To determine if aphid non-vectors respond to infection presence and severity in a
264 similar way as whitefly vectors, we carried out dual choice tests examining aphid settling
265 preferences between healthy and infected plants within each disease progression time point.
266 For each test, a pair of CYSDV-infected and sham-inoculated melon plants (either both 2 wpi
267 or 4wpi) were selected and the third leaf of the vine was presented to the aphids in a dual
268 choice arena (Supplementary Figure 3). We released 20 adult aphids (either alates or
269 apterous) into each arena from a tube screwed to the bottom of the Petri dish. Aphids were
270 allowed to settle on the exposed abaxial leaf surfaces. We counted the number of aphids
271 settled on each leaf at 1, 2 and 24h to assess initial preferences (1-2 hours) and final
272 preferences (24 hours). In total, 20-22 pairs of infected and sham-inoculated melon plants
273 were used per infection x disease progression factor combination.

274

275 ***Whitefly and aphid feeding behavior***

276 We used the DC-EPG system as previously described by (Tjallingii 1988) to investigate the
277 effects of CYSDV infection in melons on feeding behavior of the vector *B. tabaci* and non-
278 vector *A. gossypii*. To create electrical circuits that each included a plant and an insect, we
279 tethered each insect by attaching a thin wire, 2.5 μm platinum (Wollaston process wire;
280 Sigmund Cohn Corp., Mt. Vernon, New York, USA) for *B. tabaci* (Chesnais and Mauck 2018;
281 Milenovic et al. 2019) and 12.5 μm gold for *A. gossypii* (Peng and Walker 2018), to the
282 pronotum using conductive water-based silver glue. To facilitate the tethering process, non-
283 viruliferous female whiteflies were immobilized for 30-45 seconds at $-20\text{ }^{\circ}\text{C}$ in a freezer and
284 placed on a Petri dish lid that was set on top of an ice pack, under a dissecting microscope.
285 For *A. gossypii*, individuals were immobilized at the edge of a pipette tip using a vacuum
286 pump and then attached by a gold wire to the dorsum. After a 30-minute starvation period,
287 we positioned each whitefly or aphid on the abaxial face of the leaf (the preferred feeding
288 location) and inserted a second electrode into the soil of each potted plant to close the
289 electrical circuit. We recorded from eight insects simultaneously over an eight-hour period of
290 the photophase using a Giga-8 DC-EPG amplifier. Each insect-plant system was housed
291 inside a Faraday cage located in a climate-controlled room held at $24 \pm 1\text{ }^{\circ}\text{C}$. We used the
292 PROBE 3.5 software (EPG Systems, www.epgsystems.eu) to acquire and analyze EPG
293 waveforms and relevant EPG variables were calculated with EPG-Calc 6.1 software
294 (Giordanengo 2014). We chose variables based on different EPG waveforms (described by
295 (Janssen et al. 1989) for whiteflies and described by (Tjallingii and Hogen Esch 1993) for
296 aphids) corresponding to behaviors relevant to virus transmission (for whiteflies) and

297 nutrition (both insects): stylet pathways in plant tissues except phloem and xylem; salivation
298 in phloem; and passive phloem sap ingestion.

299

300 ***Plant quality assessments***

301 To determine whether CYSDV-infection affects whitefly performance, adult whiteflies were
302 collected and released into two clip-cages (~50 females per cage) on the third and fourth
303 leaves of each melon plants (either CYSDV-infected or sham-inoculated after two or four
304 wpi). Three days after infestation, the number of live females and the number of eggs laid
305 per female were determined by counting individual eggs under a stereomicroscope. Whitefly
306 oviposition is dependent on females maintaining access to sufficient nutrients and we used
307 oviposition as a proxy for performance in this study (Xu et al. 2019).

308

309 To determine the effect of CYSDV-infection on aphid performance, we evaluated population
310 growth on infected and healthy plants. Preliminary experiments indicated that leaf four of 4
311 wpi CYSDV-infected plants (that used in all other assays) frequently underwent senescence
312 in response to establishment of *A. gossypii* colonies. Therefore, we opted to evaluate
313 population growth across the time period in which plants are transitioning from 2 wpi to 4 wpi
314 (from day 18 post-inoculation to day 29 post-inoculation). To standardize cohorts of aphids
315 for experiments, we infested four young melon plants with 15 apterous and 10 alate adults
316 and allowed offspring production for 36 hours. We used the resulting offspring cohort two
317 days later for experiments (2nd-3rd instar). To infest plants, a small section of leaf with five
318 aphids present was excised and placed on the 3rd leaf from the base, which was enclosed in
319 a drawstring mesh cage that allowed access from either side (petiole and leaf tip). Aphids
320 were allowed to reproduce for eleven days (approximately 2 generations) after which we
321 counted the number present on the infested leaves. Two replicate experiments were
322 performed with 6-8 replications of each treatment within each experiment.

323

324 ***Quantification of primary metabolites and volatile emissions***

325 *Quantification of leaf primary metabolites.* To determine whether CYSDV infection and
326 disease progression modify primary metabolism, we quantified sugars and amino acids in
327 leaf tissue. We collected approximately 12-15 small (7.5mm diameter) leaf discs from in
328 between major veins, weighed the tissue, and flash froze it in liquid nitrogen before storing at
329 -80 °C. We sampled the same leaf position used in preference tests, performance tests, and
330 EPG recordings (third leaf for the earlier time point, fourth leaf for the later time point), as
331 well as the seventh leaf, which was asymptomatic in both 2 wpi and 4 wpi treatments. Both
332 lower and upper leaves from 11 CYSDV-infected plants (4wpi), 15 sham-inoculated plants
333 (4wpi), 16 CYSDV-infected plants (2wpi), and 16 sham-inoculated plants (2wpi) were

334 sampled. Leaf discs were removed from one side of the leaf for consistency, and the tip of
335 the leaf was removed for semi-quantitative ELISA (Kenney et al. 2020). Extraction and
336 derivatization of leaf metabolites was performed as previously described (Mauck et al. 2014,
337 2015) (details in Supplemental Materials). The GC-MS system used to identify and quantify
338 metabolites consisted of a Thermo Scientific Trace 1310 gas chromatograph coupled with an
339 AI 1310 autosampler and a TSQ Duo triple quadrupole mass spectrometer. Data acquisition
340 and processing were controlled by Chromeleon 7 software (GC-MS parameters and
341 quantifications in Table 1).

342

343 *Volatile collection and quantification by gas chromatography and mass spectrometry.* For
344 volatile collections, we focused on assaying sham-inoculated and CYSDV-infected plants at
345 four weeks post-inoculation, as infection at this time point elicited whitefly attraction in
346 assays permitting access to all cues, but infection at two weeks post-inoculation did not.
347 Eight CYSDV-infected plants and 6 sham-inoculated plants were used. Volatile collections
348 were performed using a push-pull volatile sampling system, with 2 L per minute of charcoal-
349 filtered clean air pushed into 7.5 L jars enclosing symptomatic portions of plants, and
350 corresponding plant portions on sham-inoculated plants. We cleaned jars and teflon
351 guillotine bases with zero-residue ammonia-based soap, distilled water, and rinses of
352 acetone and hexanes, respectively. Volatiles were sampled by pulling headspace air across
353 a trap containing 40mg of Hayesep-Q adsorbent (Mesh 80-100, Hayes Separations, Inc.) at
354 a rate of 1 L per minute. Collections were performed during the photophase (11:00-17:00).
355 We eluted volatiles from traps with 150uL of dichloromethane (Acros Organics 326600025)
356 spiked with 600 ng of nonyl acetate (Sigma Aldrich W278807-SAMPLE) and 300 ng of n-
357 octane (Sigma Aldrich 74820-5ML) as internal standards. Blank collections were also
358 performed to account for any trace background contaminants. We used the GC-MS system
359 described above for volatile identification and quantification (settings in Table 2).

360

361 **Statistical analyses**

362 Data on whitefly settling preference were analyzed using approximate Friedman tests on
363 responding whiteflies. When a significant effect was detected, a pairwise comparison using
364 Wilcoxon signed rank test (P -value adjustment with “holm” method) at the 0.05 significance
365 level was used to test for differences between treatments. The whitefly settling rates varied
366 irregularly with the leaf color (percentage of yellow), and we therefore analysed the data with
367 a generalised additive model (GAM; “mgcv” package (Wood 2017)) with “yellow” as a
368 smoothed predictor. The error distribution and model fit were checked with the gam.check
369 function. Data on whitefly volatile-based preference were analyzed using a paired t-test.
370 Data on aphid settling preferences were analyzed using Wilcoxon signed rank test. We used

371 generalized linear models (GLM) with a likelihood ratio and Chi-square test to assess
372 whether there was an effect of plant infection status on both *B. tabaci* and *A. gossypii*
373 feeding behaviors. We included the CYSDV infection status (“virus”) and weeks post-
374 inoculation (“week”) as main factors and also studied their interaction (“virus:week”). Data on
375 feeding behavior (probing and phloem sap ingestion phases) was not normally distributed,
376 accordingly we carried out a GLM using a Gamma (link = “inverse”) distribution. When a
377 significant effect of one of the main factors was detected or when an interaction between
378 factors was significant, a pairwise comparison using Estimated Marginal means (package R:
379 “emmeans”) (*P*-value adjustment with Tukey method) at the 0.05 significance level was used
380 to test for differences between treatments.

381

382 Data on whitefly (and aphid) performance were not normally distributed (count data),
383 and accordingly, were analyzed using a generalized linear model (GLM) with errors modeled
384 using a Poisson distribution. A quasi-likelihood function was used to correct for
385 overdispersion, and Log was specified as the link function in the model. We included “plant
386 infection”, “session” and “clip-cage” as main factors and also studied their interaction. The fit
387 of all generalized linear models was checked by inspecting residuals and QQ plots. For
388 carbohydrate metabolites, we analyzed compounds separately by leaf position using general
389 linear models, with “plant infection” and “week post inoculation” as factors and post-hoc
390 Tukey tests for significant main effects. Most compounds required log transformation to meet
391 normality assumptions of the model. Mean values are reported with the standard errors of
392 the means (SEM) and sample sizes in ensuing figures. To test if the different factors “plant
393 infection”, “week post inoculation” and “leaf position” explain a significant proportion in amino
394 acid composition and quantity variations, we used a Redundancy Analysis (RDA) following
395 the procedure described in Hervé et al. (2020) (see ESM for full details). To test if the
396 infection explains plant volatiles emissions, we used a PPLS-DA procedure as described in
397 (Hervé et al. 2018) (see ESM for full details). Plant volatile blends were log transformed
398 before PPLS-DA and the significance of the treatment was assessed using a permutation
399 analysis (999 repetitions) implemented in the MVA.test from the RVAideMemoire package.
400 As a follow-up, we used a decision-tree-based method ‘Random Forest’ (RF) for variable
401 selection to detect the most important compounds that account for significant differences
402 (see ESM for full details). We used out-of-bag (OOB) error rates as the importance score for
403 variable selection implemented as backward elimination in the package varSelRF.
404 Performance of the RF models was evaluated by the misclassification error rate. All
405 statistical analyses were performed using Minitab v. 14 or R software (version 4.0.2) (R Core
406 Team 2020).

407

408 Results

409 *Whitefly and aphid preference tests*

410 Responding whiteflies preferentially settled on 4wpi CYSDV-infected melon leaves after 1h,
 411 2h and 24h (Approximate Friedman tests, $P < 0.001$) (Fig. 1). To a lesser extent, whiteflies
 412 also preferred to settle on the 4wpi sham-inoculated leaves over 2 wpi sham-inoculated
 413 leaves. The number of responding whiteflies increased gradually, from 70% after 1 hour to
 414 over 90% after 24 hours. Whitefly settling on 4 wpi CYSDV-infected was positively affected
 415 by leaf symptoms (yellow discoloration) up until a discoloration of ~70% then the preference
 416 is reduced (GAM model, $F = 8.097$; estimated $df = 7.143$; $P < 0.001$; $R\text{-sq}(adj) = 0.763$) (Fig.
 417 2a). A complementary bioassay presenting only volatile cues in the absence of treatment-
 418 specific visual or contact cues indicates that whitefly preferences for 4 wpi CYSDV-infected
 419 plants are not driven by odors (Student t-test, $t = 0.91$, $P = 0.376$) (Fig. 2b).

420
 421 CYSDV-infection on 2 wpi melon leaves did not significantly influence apterous and alate
 422 aphid settlement preference after 1, 2 and 24 hours (Wilcoxon signed rank tests, $P > 0.05$)
 423 (Fig. 3a). Alate aphids exhibited a slight preference for sham-inoculated leaves over 4 wpi
 424 CYSDV-infected melon leaves at 1 hour and after 24 hours (Wilcoxon signed rank test, $V =$
 425 34.5 , $P = 0.015$ and $V = 21.5$, $P = 0.003$, respectively) while apterous aphids settled evenly
 426 on both sham-inoculated and CYSDV-infected leaves (Wilcoxon signed rank tests, $P > 0.05$)
 427 (Fig. 3b). The number of responding aphids, either apterous or alatae, increased gradually
 428 from 80% after 1 hour to over 90% after 24 hours.

429

430 *Whitefly and aphid feeding behavior*

431 For whiteflies, the durations of pathway phases and salivation in phloem on melon plants
 432 were not affected by CYSDV-infection at both 2 wpi and 4 wpi time points (GLM, “virus”: $P =$
 433 0.723 , “week”: $P = 0.052$, interaction “virus:week”: $P = 0.085$ and “virus”: $P = 0.677$, “week”:
 434 $P = 0.104$, interaction “virus:week”: $P = 0.793$, for pathway and salivation phases,
 435 respectively) (Fig. 4a). However, whiteflies performed longer phloem sap ingestion on
 436 CYSDV-infected melon plants regardless of the stage of disease progression (GLM, “virus”:
 437 $P = 0.011$, “week”: $P = 0.579$, interaction “virus:week”: $P = 0.537$) (Fig. 4a) (see ESM for
 438 detailed Table S2).

439

440 For *A. gossypii*, durations of pathway phases melon plants were increased on
 441 CYSDV-infected plants in both the 2 wpi and 4 wpi time points (GLM, “virus”: $P = 0.001$,
 442 “week”: $P = 0.475$, interaction “virus:week”: $P = 0.263$) (Fig. 4b). Aphids performed longer
 443 salivation phases in phloem at 4 wpi time point (GLM, “virus”: $P < 0.001$, “week”: $P = 0.373$,
 444 interaction “virus:week”: $P = 0.589$). However, aphids performed shorter phloem sap

445 ingestions on CYSDV-infected melon plants in both time points (GLM, “virus”: $P = 0.002$,
 446 “week”: $P = 0.509$, interaction “virus:week”: $P = 0.332$) (Fig. 4b).

447

448 **Plant quality assessments**

449 Whitefly fecundity on CYSDV-infected melon plants was reduced by 20-30% after feeding on
 450 plants in both the 2 wpi (GLM, $\chi^2 = 12.075$, $P < 0.001$) (Fig. 5a) and 4 wpi time points (GLM,
 451 $\chi^2 = 4.091$, $P < 0.043$) (Fig. 5b). We observed an effect of the repetition for both 2 weeks
 452 post-inoculation (GLM, $\chi^2 = 29.127$, $P < 0.001$) and 4 weeks post-inoculation fertility
 453 experiments (GLM, $\chi^2 = 7.098$, $P = 0.008$). At 4 weeks post-inoculation, the fertility of
 454 whiteflies was higher on the third leaf than the fourth leaf (factor: “clip-cage”) (GLM, $\chi^2 =$
 455 6.125 , $P = 0.013$).

456

457 Population growth for *Aphis gossypii* on CYSDV-infected plants was significantly
 458 reduced relative to sham-inoculated plants during the transition from 2 wpi to 4 wpi (GLM, χ^2
 459 $= 494.7$, $P < 0.001$) (Fig. 6). Significant temporal effects were also detected, with higher
 460 aphid fecundity during the second replication of the experiment relative to the first (GLM, $\chi^2 =$
 461 5209.1 , $P < 0.001$). Aphids established on the fourth leaf of 4 wpi CYSDV-infected plants
 462 elicited rapid senescence in the leaf tissue; most infected leaves became unsuitable early on
 463 in the experiment (6/8), but most sham-inoculated leaves (5/6) continued to support aphids
 464 until day 11 post-infestation (data not shown).

465

466 **Quantification of primary metabolites and volatile emissions**

467 We detected glucose, fructose, and sucrose as well as sixteen proteinogenic amino acids in
 468 the analysis of primary metabolites in leaf tissue (Fig. 7a, Table S3 and S4 in ESM). For
 469 upper leaves (asymptomatic in both disease progression stages), sucrose concentration was
 470 influenced by infection status (GLM, $F = 4.49$, $P = 0.039$) and time point (wpi for infected and
 471 weeks post sham-inoculation for controls) (GLM, $F = 13.50$, $P = 0.001$) but not by their
 472 interaction (Fig. 7a). Glucose concentration in upper leaves was influenced by time point
 473 (GLM, $F = 8.12$, $P = 0.006$), with infection status marginally non-significant (GLM, $F = 3.78$,
 474 $P = 0.057$) (Fig. 7c). Fructose concentration in upper leaves was influenced by infection
 475 status (GLM, $F = 6.89$, $P = 0.011$) with a significant interactions of infection status and time
 476 point (GLM, $F = 5.57$, $P = 0.022$) and a marginally non-significant effect of time point (GLM,
 477 $F = 3.49$, $P = 0.067$) (Fig. 7e). For lower leaves (symptomatic in 4 wpi and asymptomatic in 2
 478 wpi treatment groups) sucrose concentration was significantly influenced by time point
 479 (GLM, $F = 10.34$, $P = 0.002$) (Fig. 7b). There was a marginally non-significant trend of time
 480 point having an effect on glucose concentration (GLM, $F = 3.88$, $P = 0.054$) with a significant
 481 interaction between infection status and time point (GLM, $F = 4.08$, $P = 0.048$) (Fig. 7d).

482 Fructose concentration was significantly influenced by time point (GLM, $F = 6.80$, $P = 0.012$)
483 and the interaction of infection status and time point (GLM, $F = 9.02$, $P = 0.004$) (Fig. 7f).

484

485 Redundancy analysis with permutation testing indicates that the main drivers of
486 variation in leaf amino acid composition (consisting of compound identity and quantity) are
487 the time point at which the samples are taken (2 wpi vs. 4 wpi, $F = 9.49$, $P = 0.001$) and the
488 leaf position (upper vs. lower, $F = 5.81$, $P = 0.001$) (Table 3). We also detected a significant
489 interaction between infection status and time point ($F = 3.08$, $P = 0.004$), a significant
490 interaction between infection status and leaf position ($F = 2.43$, $P = 0.017$), and a significant
491 interaction between time point and leaf position ($F = 3.57$, $P = 0.003$) (Table 3). Constrained
492 ordination plots (Fig. 8) illustrate clustering of treatment groups based on significant and
493 marginally non-significant interaction effects.

494 Volatile collections were only performed for the time point in which we detected
495 significant differences in whitefly preferences among infected and non-infected hosts (4 wpi).
496 Blend compositions (compound identities and quantities) were analyzed using PPLS-DA,
497 which detected significant differences in blends based on the infection status factor (CER =
498 14.3%, $P = 0.002$). The first two ordination axes explained 78.13% (44.16% and 33.97%
499 respectively) of variation in volatile blends and clearly separated infected from sham-
500 inoculated plants (Fig. 9a). A complementary random forest analysis also clearly separated
501 treatments based on blend features (out-of-bag error rate 28.57%, Fig. 9b) and identified two
502 compounds that were strong predictors of infection status (3-hexen-1-ol and 4-hexen-1-ol,
503 isomers not discernible).

504 Discussion

505 Repeated documentation of transmission-conducive phenotypic changes in hosts has led to
506 the hypothesis that plant viruses evolve specific adaptations for “manipulating” host-vector
507 interactions to facilitate their own transmission (Mauck et al. 2012, 2018; Eigenbrode et al.
508 2017). However, the taxonomic diversity of viruses examined for evidence of manipulative
509 effects remains limited, with many emerging pathogens of concern not yet studied.
510 Additionally, limited evidence suggests that effects of viruses on their hosts and vectors are
511 not static, but change over the course of plant phenology and disease progression (Werner
512 et al. 2009; Rajabaskar et al. 2013; Lu et al. 2016; Shrestha et al. 2019). “Manipulations” can
513 also change how hosts resist abiotic stressors and interact with other, non-vector organisms
514 (Davis et al. 2015; Mauck et al. 2015). Thus, to determine whether putative virus
515 manipulations are biologically meaningful in managed and unmanaged communities, we
516 must begin to consider virus-induced phenotypes in a broader ecological context.

517 Our results indicate that CYSDV induces changes in *C. melo*, its main agricultural
518 host, that are consistent with host and vector manipulation: CYSDV infection significantly
519 increased whitefly settling and phloem sap uptake. Given that CYSDV is only acquired and
520 inoculated from the phloem, these effects should increase both the number of viruliferous
521 whiteflies on infected hosts and the probability of each whitefly obtaining sufficient virions to
522 subsequently inoculate (Ng and Zhou 2015). Virus-induced phenotypes and their effects
523 on vector behavior were also strongly influenced by the stage of disease progression, with
524 the most pronounced transmission-conducive phenotype evident at 4 wpi (increased
525 attraction and phloem sap uptake) relative to 2 wpi (only increased phloem sap uptake). This
526 finding lends further support to a growing body of evidence that virus effects on host
527 phenotypes and vector behavior are not static (Blua and Perring 1992a, b; Shrestha et
528 al. 2019), but change dynamically over time, with significant implications for virus evolution
529 and management (Mauck and Chesnais 2020).

530 Even though whiteflies preferred and fed more easily on infected hosts, whitefly
531 females produced fewer eggs on infected plants in both stages of disease progression
532 during no-choice feeding trials. Although this may appear to be detrimental for the virus, on
533 the contrary, lower host quality may encourage whiteflies to emigrate after feeding for long
534 enough to become viruliferous. This finding highlights the insights we can gain from studying
535 viruses with semi-persistent transmission modes; as a semi-persistent virus, prolonged
536 feeding and settling on infected hosts after virus acquisition is more likely to hinder rather
537 than enhance new CYSDV infections (Ng and Zhou 2015). And mathematical models have
538 shown that the benefits of attracting and retaining vectors depend on there being a
539 mechanism for dispersal through a reversal of the preference for infected hosts (Roosien et
540 al. 2013; Shaw et al. 2017). Although we did not observe defection in the 24-hour time frame
541 of our tests, the fecundity measurements suggest that a slower-acting, inducible antibiosis
542 may encourage later dispersal. An interesting next step in studying the CYSDV-melon
543 pathosystem would be to perform further experiments that quantify post-acquisition effects of
544 CYSDV on vector behavior (Chesnais et al. 2020), as well as effects of vector feeding on the
545 expression of virus-induced phenotypes.

546 Parallel experiments showed that the same symptoms that induce greater visitation
547 and settling by whiteflies on infected hosts had opposite effects on the behavior of a non-
548 vector competitor (*A. gossypii*), even though both whiteflies and aphids must locate and
549 ingest nutrients from the same host tissue (phloem elements). Regardless of the time point
550 in disease progression, *A. gossypii* was largely indifferent to disease status in free choice
551 tests, with a slight preference for sham-inoculated plants. EPG recordings revealed that this

552 preference may be linked to greater difficulty in feeding on infected plants during both
553 asymptomatic and symptomatic disease stages. Subsequent aphid performance
554 experiments carried out across the transition from the asymptomatic to symptomatic
555 condition indicate that this difficulty in feeding (antixenosis) may contribute to reductions in
556 fecundity and overall aphid population size on infected relative to non-infected hosts.

557 Reduced feeding and reproduction by *A. gossypii* is biologically significant because it
558 suggests dual benefits of the CYSDV-induced host phenotype for the virus: attraction and
559 retention of vectors plus repellence and resistance against a damaging non-vector that
560 competes directly with the vector. We previously documented a similar effect of infection by
561 *Cucumber mosaic virus* (CMV) (family *Bromoviridae*, genus *Cucumovirus*) on non-vector
562 herbivores of squash; phenotypic changes that encourage virion acquisition and dispersal by
563 vectors also discourage feeding and oviposition by non-vector herbivores (Mauck et al.
564 2015). Based on this work, we hypothesized that virus-induced changes that reduce damage
565 from herbivores are conducive to transmission because infected hosts will remain in the
566 landscape for longer periods of time and continue to serve as sources of inoculum (Mauck et
567 al. 2015, 2018). By exploring impacts of CYSDV infection on host interactions with a non-
568 vector, we provide evidence that a virus can induce a phenotype that both facilitates
569 transmission-conducive interactions with vectors and hinders feeding and exploitation by a
570 non-vector.

571 Our selected plant trait analyses provided insight into the mechanisms underlying
572 CYSDV effects on hosts, vectors, and non-vectors, but do not provide a complete
573 explanation for all observed patterns. CYSDV infection induced changes in both leaf volatiles
574 and leaf appearance (degree of yellowing) at the most attractive time point (4wpi). However,
575 whiteflies exhibited no preference for 4wpi infected hosts based on odor cues alone, while
576 the number of whiteflies selecting 4wpi infected hosts when color cues were accessible was
577 more than twice the number choosing sham inoculated hosts of the same age, or
578 asymptomatic 2wpi infected hosts. When we analyzed the relationship between the degree
579 of symptom severity (yellowing) and whitefly preference (percentage selecting that leaf)
580 using a subset of the data that included only 4wpi infected hosts, we detected a tight
581 relationship between the percentage of yellowing and whitefly settling. Although we did not
582 focus on 2wpi hosts for volatile analysis, it should be noted that there was also a slight
583 preference for leaves of 4wpi sham-inoculated plants over leaves of 2wpi sham-inoculated
584 plants in preference tests. We suspect this preference is also driven by slight color
585 differences between the older leaves of 4wpi sham plants, which we observed to be a lighter
586 green color relative to darker green leaves in the same vine position on 2wpi sham plants. In

587 future experiments, it would be interesting to use plant age and infection status as a basis for
588 further dissecting the relative importance of different types of cues used by whiteflies under
589 varying conditions. Overall, whitefly preferences in our experiments are consistent with
590 prior studies documenting strong whitefly attraction to the color yellow (Coombe 1981;
591 Stukenberg and Poehling 2019) with yellow or yellow-green traps being a primary means of
592 whitefly monitoring in agricultural settings (Berlinger and Others 1980; Gillespie and Quiring
593 1987).

594 Our results are also congruent with those of another study documenting effects of
595 a related crinivirus, *Tomato chlorosis virus* (ToCV) (family *Closteroviridae*, genus *Crinivirus*)
596 on vision-based preferences and odor-based preferences of *B. tabaci* (Fereres et al.
597 2016). This study reported attraction of non-viruliferous whiteflies to ToCV-infected
598 tomato plants based on visual cues presented in the absence of contact or odor cues
599 (Fereres et al. 2016). When only odor cues were permitted, non-viruliferous whiteflies were
600 instead slightly repelled by odors of ToCV-infected plants. Like CYSDV, ToCV induces
601 yellowing of host foliage when infecting highly susceptible crops but does not cause rugosity
602 (wrinkling/puckering) leaf rolling, or other size reductions (Wintermantel and Wisler 2006).
603 The study by Fereres et al. (2016) suggests that ToCV-infected tomato plants exhibit
604 symptoms that are visually attractive and do not suffer decreased apparency
605 due to severe reductions in size or leaf area. However, a follow-up study using near-identical
606 plant ages and culture conditions (Maluta et al. 2017) found that non-viruliferous whitefly
607 preferences for ToCV-infected tomatoes were reversed when access to all cues (visual,
608 odor, and contact) was permitted. Additionally, both studies found that whitefly preferences
609 often depend on viruliferous status, even when the virus being acquired (ToCV) does not
610 enter and circulate in insect hemolymph. Thus, the relative importance of different cues may
611 vary across situations, vector conditions, and bioassay designs. This will be important to
612 consider in future efforts to extrapolate results for ToCV or CYSDV to whole plants in field
613 settings.

614 Although it is difficult to clarify the relative importance of different cues in the
615 laboratory, the benefits, for the virus, of manipulating leaf appearance are readily
616 apparent when you consider that whiteflies are minute and poor flyers. In a field
617 environment, volatile blends are less likely to be constant across the space between a
618 vector and an infected plant (Byrne et al. 1988; Byrne 1999; Aartsma et al. 2017). Virus-
619 induced changes in volatiles are also more subject to perturbations due to feeding by other
620 organisms or co-occurring pathogens (Salvaudon et al. 2013) as well as abiotic conditions
621 (Blanc and Michalakakis 2016). In contrast, a visual source remains fixed in space and, to

622 some degree, more constant over time. This is the case for CYSDV infection in melons;
623 yellowing becomes apparent 21-28 days after successful inoculation and this phenotype
624 (represented by our 4 wpi time point) persists for weeks (Wintermantel et al. 2017). Based
625 on the present results, we hypothesize that changes in visual cues are an essential
626 component of virus manipulations that enhance whitefly attraction to infected hosts.
627 Disrupting these changes may be a viable route for reducing virus spread in agricultural
628 settings (Kenney et al. 2020).

629 Our study also quantified changes in primary metabolites associated with infection
630 status, disease progression, and leaf age within disease and time point categories.
631 Surprisingly, these analyses did not reveal any strong connections among drivers of
632 variation in leaf tissue metabolites, vector and non-vector behavioral preferences, and stylet
633 activities inside plant tissues. Amino acid composition and quantities varied primarily based
634 on time point (2wpi vs. 4wpi), with little separation based on infection status. Leaf sugar
635 concentrations also varied based on time point: for both upper and lower leaves, glucose,
636 fructose, and sucrose were higher in leaves of 4wpi vs. 2wpi sham-inoculated plants. The
637 most significant change due to CYSDV infection was increased variation in sugar quantities
638 and nullification of differences between the 2wpi and 4wpi time points; glucose,
639 fructose and sucrose quantities in 2wpi infected plants do not differ from those in 4wpi
640 infected plants, but all three compounds are significantly different by time point for sham-
641 inoculated plants. While this is interesting, there is no clear connection to the outcomes of
642 behavior experiments. For example, in choice tests, whiteflies exhibited only a slight
643 preference for 4wpi sham-inoculated plants over 2wpi sham-inoculated plants. This outcome
644 could be partially driven by the higher quantities of sugars in leaf tissues, or a combination of
645 differences in sugar quantities and amino acid composition. But differences in stylet activities
646 consistent with metabolites being involved in this preference were not evident in whitefly
647 EPG experiments. And aphid stylet activities were similarly unaffected by the time point, with
648 CYSDV infection status being the only significant term in the model. Collectively, these
649 results show that the two hemipterans studied here are not strongly responsive to the
650 range of variation in melon leaf tissue primary metabolites we observed.

651 Based on this, we hypothesize that primary metabolic pathways in leaves are not
652 targets for manipulation by CYSDV and that the phenotypes observed manifest via
653 mechanisms not explored in our study. We observed most post-contact behavioral effects
654 (e.g., EPG) over short time frames (a few hours), suggesting that the phenotype underlying
655 these effects may involve changes initiated by infection prior to vectors contacting infected
656 hosts rather than a slow activation of defenses over time following vector feeding. Effects of

657 this sort could be mediated by constitutively produced compounds not measured in this
658 study and by changes in plant architecture. There is some evidence for the latter mechanism
659 from prior work on CYSDV pathology. In *C. melo*, CYSDV virions are present in phloem
660 sieve elements, as well as phloem parenchyma, bundle sheath, and companion cells. Within
661 these tissues, infection can induce vesicles, cell wall overgrowths, lipid bodies,
662 plasmalemma deposits and cytopathological effects on organelles, particularly chloroplasts
663 and mitochondria (Medina et al. 2003). Thus, CYSDV and other criniviruses possess
664 adaptations for inducing drastic changes in the architecture of cells that form the interface
665 between the site of nutrient acquisition for whiteflies and aphids (sieve elements) and the
666 tissue that must be bypassed to reach this site (mesophyll). The importance of focusing on
667 these mechanisms in future work was directly revealed by our comparative approach
668 exploring behavior of two hemipterans in the context of metabolomics.

669 Overall, our study makes several important contributions to our understanding of the
670 ecology of plant virus manipulation of host phenotypes and vector behavior in monoculture
671 crops. We found that CYSDV infection discourages colonization by a non-vector competitor
672 while inducing a suite of changes that encourage virion acquisition from infected hosts by the
673 vector, with the most effective manipulation occurring at the latter stage of disease
674 progression due to the appearance of a visually attractive phenotype. This same phenotype
675 is characteristic of infections in the field (Wintermantel et al. 2017) and can be disrupted by
676 manipulating host resistance and tolerance to infection with commercially available plant
677 defense priming agents (Kenney et al. 2020). Thus, our study has the potential to directly
678 inform management options that target a putative virus manipulation of vector behavior. It
679 also provides new insight into the hierarchies of cues used by different phloem-feeding
680 Hemipterans and the ways that virus infection alters vector-competitor interactions.
681 Importantly, this knowledge, and its potential for real-world applications, would not have
682 been discovered if we focused solely on behavioral responses of only vectors at a single
683 time point in disease progression.

684

685 **References**

- 686 Aartsma Y, Bianchi FJ, van der Werf W, et al (2017) Herbivore-induced plant volatiles and
687 tritrophic interactions across spatial scales. *New Phytol* 216:1054–1063
- 688 Ángeles-López YI, Rivera-Bustamante R, Heil M (2017) Fatal attraction of non-vector
689 impairs fitness of manipulating plant virus. *J Ecol* 38:251. <https://doi.org/10.1111/1365-2745.12838>
- 691 Bak A, Patton MF, Perilla-Henao LM, et al (2019) Ethylene signaling mediates potyvirus

- 692 spread by aphid vectors. *Oecologia*. <https://doi.org/10.1007/s00442-019-04405-0>
- 693 Belliure B, Sabelis MW, Janssen A (2010) Vector and virus induce plant responses that
694 benefit a non-vector herbivore. *Basic Appl Ecol* 11:162–169.
695 <https://doi.org/10.1016/j.baae.2009.09.004>
- 696 Berlinger MJ, Others (1980) A yellow sticky trap for whiteflies: *Trialeurodes vaporariorum*
697 and *Bemisia tabaci* (Aleyrodidae). *Entomol Exp Appl* 27:98–102
- 698 Blanc S, Michalakakis Y (2016) Manipulation of hosts and vectors by plant viruses and impact
699 of the environment. *Current Opinion in Insect Science* 16:36–43.
700 <https://doi.org/10.1016/j.cois.2016.05.007>
- 701 Blua MJ, Perring TM (1992a) Effects of Zucchini yellow mosaic virus on colonization and
702 feeding behavior of *Aphis gossypii* (Homoptera: Aphididae) alatae. *Environ Entomol*
703 21:578–585. <https://doi.org/10.1093/ee/21.3.578>
- 704 Blua MJ, Perring TM (1992b) Alatae production and population increase of aphid vectors on
705 virus-infected host plants. *Oecologia* 92:65–70. <https://doi.org/10.1007/BF00317263>
- 706 Byrne DN (1999) Migration and dispersal by the sweet potato whitefly, *Bemisia tabaci*. *Agric*
707 *For Meteorol* 97:309–316
- 708 Byrne DN, Buchmann SL, Spangler HG (1988) Relationship between wing loading, wingbeat
709 frequency and body mass in homopterous insects. *J Exp Biol* 135:9–23
- 710 Capinera JL (2009) *Aphis gossypii* Glover (Insecta: Hemiptera: Aphididae). In: University of
711 Florida, Entomology and Nematology.
712 http://entnemdept.ufl.edu/creatures/veg/aphid/melon_aphid.htm. Accessed 12 Aug 2020
- 713 Celix A, Lopez-Sese A, Almarza N, et al (1996) Characterization of cucurbit yellow stunting
714 disorder virus, a *Bemisia tabaci*-transmitted Closterovirus. *Phytopathology* 86:1370–
715 1376
- 716 Chesnais Q, Caballero Vidal G, Coquelle R, et al (2020) Post-acquisition effects of viruses
717 on vector behavior are important components of manipulation strategies. *Oecologia*
718 194:429–440. <https://doi.org/10.1007/s00442-020-04763-0>
- 719 Chesnais Q, Mauck KE (2018) Choice of tethering material influences the magnitude and
720 significance of treatment effects in whitefly electrical penetration graph recordings. *J*
721 *Insect Behav* 1–16. <https://doi.org/10.1007/s10905-018-9705-x>
- 722 Coombe PE (1981) Wavelength specific behaviour of the whitefly *Trialeurodes vaporariorum*
723 (Homoptera: Aleyrodidae). *J Comp Physiol* 144:83–90.
724 <https://doi.org/10.1007/BF00612801>
- 725 Cui N, Lu H, Wang T, et al (2019) Armet, an aphid effector protein, induces pathogen
726 resistance in plants by promoting the accumulation of salicylic acid. *Philos Trans R Soc*
727 *Lond B Biol Sci*. <https://doi.org/10.1098/rstb.2018.0314>
- 728 Davis TS, Bosque-Pérez NA, Foote NE, et al (2015) Environmentally dependent host-
729 pathogen and vector-pathogen interactions in the Barley yellow dwarf virus
730 pathosystem. *J Appl Ecol* 52:1392–1401. <https://doi.org/10.1111/1365-2664.12484>
- 731 Eigenbrode SD, Bosque-Pérez N, Davis TS (2017) Insect-borne plant pathogens and their
732 vectors: ecology, evolution, and complex interactions. *Annu Rev Entomol* 63:169–191.
733 <https://doi.org/10.1146/annurev-ento-020117-043119>

- 734 Erb M, Reymond P (2019) Molecular interactions between plants and insect herbivores.
735 *Annu Rev Plant Biol* 70:527-57. <https://doi.org/10.1146/annurev-arplant-050718-095910>
- 736 Ertunc F (2020) Chapter 46 - Emerging Plant Viruses. In: Ennaji MM (ed) *Emerging and*
737 *Reemerging Viral Pathogens*. Academic Press, pp 1041–1062
- 738 Fereres A, Peñafior MFGV, Favaro CF, et al (2016) Tomato infection by whitefly-transmitted
739 circulative and non-circulative viruses induce contrasting changes in plant volatiles and
740 vector behaviour. *Viruses* 8.: <https://doi.org/10.3390/v8080225>
- 741 Gillespie DR, Quiring D (1987) Yellow sticky traps for detecting and monitoring greenhouse
742 whitefly (Homoptera: Aleyrodidae) adults on greenhouse tomato crops. *J Econ Entomol*
743 80:675–679. <https://doi.org/10.1093/jee/80.3.675>
- 744 Giordanengo P (2014) EPG-Calc: a PHP-based script to calculate electrical penetration
745 graph (EPG) parameters. *Arthropod Plant Interact* 8:163–169.
746 <https://doi.org/10.1007/s11829-014-9298-z>
- 747 González R, Butković A, Elena SF (2020) From foes to friends: Viral infections expand the
748 limits of host phenotypic plasticity. *Adv Virus Res* 106:85–121.
749 <https://doi.org/10.1016/bs.aivir.2020.01.003>
- 750 Hervé MR, Nicolè F, Lê Cao K-A (2018) Multivariate analysis of multiple datasets: a practical
751 guide for chemical ecology. *J Chem Ecol*. <https://doi.org/10.1007/s10886-018-0932-6>
- 752 He XC, Xu HX, Zheng XS, et al (2012) Ecological fitness of non-vector planthopper
753 *Sogatella furcifera* on rice plants infected with rice black streaked dwarf virus. *Rice Sci*
754 19:335–338. [https://doi.org/10.1016/S1672-6308\(12\)60059-6](https://doi.org/10.1016/S1672-6308(12)60059-6)
- 755 Himler AG, Adachi-Hagimori T, Bergen JE, et al (2011) Rapid spread of a bacterial symbiont
756 in an invasive whitefly is driven by fitness benefits and female bias. *Science* 332:254–
757 256. <https://doi.org/10.1126/science.1199410>
- 758 Janssen JAM, Tjallingii WF, van Lenteren JC (1989) Electrical recording and ultrastructure of
759 stylet penetration by the greenhouse whitefly. *Entomol Exp Appl* 52:69–81.
760 <https://doi.org/10.1007/BF00163943>
- 761 Johnston N, Martini X (2020) The influence of visual and olfactory cues in host selection for
762 *Bemisia tabaci* Biotype B in the presence or absence of tomato yellow leaf curl virus.
763 *Insects* 11.: <https://doi.org/10.3390/insects11020115>
- 764 Kaloshian I, Walling LL (2016) Plant immunity: connecting the dots between microbial and
765 hemipteran immune responses. In: Czosnek H, Ghanim M (eds) *Management of Insect*
766 *Pests to Agriculture*. Springer International Publishing, pp 217–243
- 767 Kenney JR, Grandmont M-E, Mauck KE (2020) Priming melon defenses with acibenzolar-S-
768 methyl attenuates infections by phylogenetically distinct viruses and diminishes vector
769 preferences for infected hosts. *Viruses* 12:257. <https://doi.org/10.3390/v12030257>
- 770 Kersch-Becker MF, Thaler JS (2014) Virus strains differentially induce plant susceptibility to
771 aphid vectors and chewing herbivores. *Oecologia* 174:883–892.
772 <https://doi.org/10.1007/s00442-013-2812-7>
- 773 Lu G, Zhang T, He Y, Zhou G (2016) Virus altered rice attractiveness to planthoppers is
774 mediated by volatiles and related to virus titre and expression of defence and volatile-
775 biosynthesis genes. *Sci Rep* 6:38581. <https://doi.org/10.1038/srep38581>

- 776 Maluta NKP, Fereres A, Lopes JRS (2017) Settling preferences of the whitefly vector
777 *Bemisia tabaci* on infected plants varies with virus family and transmission mode.
778 Entomol Exp Appl 165:138–147. <https://doi.org/10.1111/eea.12631>
- 779 Maluta NKP, Fereres A, Lopes JRS (2019) Plant-mediated indirect effects of two viruses
780 with different transmission modes on *Bemisia tabaci* feeding behavior and fitness. J
781 Pest Sci 92: 405–416. <https://doi.org/10.1007/s10340-018-1039-0>
- 782 Matkin OA, Chandler PA (1957) The UC-type soil mixes. In: Baker KF (ed) The U.C. System
783 for Producing Healthy Container-grown Plants Through the Use of Clean Soil, Clean
784 Stock, and Sanitation. University of California, Division of Agricultural Sciences, pp 68–
785 85
- 786 Mauck KE, De Moraes CM, Mescher MC (2010) Deceptive chemical signals induced by a
787 plant virus attract insect vectors to inferior hosts. Proc Natl Acad Sci USA 107:3600–
788 3605. <https://doi.org/10.1073/pnas.0907191107>
- 789 Mauck KE, Bosque-Pérez NA, Eigenbrode SD, et al (2012) Transmission mechanisms
790 shape pathogen effects on host-vector interactions: evidence from plant viruses. Funct
791 Ecol 26:1162–1175. <https://doi.org/10.1111/j.1365-2435.2012.02026.x>
- 792 Mauck KE, Chesnais Q (2020) A synthesis of virus-vector associations reveals important
793 deficiencies in studies on host and vector manipulation by plant viruses. Virus Res
794 285:197957. <https://doi.org/10.1016/j.virusres.2020.197957>
- 795 Mauck KE, Chesnais Q, Shapiro LR (2018) Evolutionary determinants of host and vector
796 manipulation by plant viruses. Adv Virus Res 101:189–250.
797 <https://doi.org/10.1016/bs.aivir.2018.02.007>
- 798 Mauck KE, De Moraes CM, Mescher MC (2016) Effects of pathogens on sensory-mediated
799 interactions between plants and insect vectors. Curr Opin Plant Biol 32:53–61.
800 <https://doi.org/10.1016/j.pbi.2016.06.012>
- 801 Mauck KE, De Moraes CM, Mescher MC (2014) Biochemical and physiological mechanisms
802 underlying effects of Cucumber mosaic virus on host-plant traits that mediate
803 transmission by aphid vectors. Plant Cell Environ 37:1427–1439.
804 <https://doi.org/10.1111/pce.12249>
- 805 Mauck KE, Kenney J, Chesnais Q (2019) Progress and challenges in identifying molecular
806 mechanisms underlying host and vector manipulation by plant viruses. Current Opinion
807 in Insect Science 33:7–18. <https://doi.org/10.1016/j.cois.2019.01.001>
- 808 Mauck KE, Smyers E, De Moraes CM, Mescher MC (2015) Virus infection influences host
809 plant interactions with non-vector herbivores and predators. Funct Ecol 29:662–673.
810 <https://doi.org/10.1111/1365-2435.12371>
- 811 Medina V, Rodrigo G, Tian T, et al (2003) Comparative cytopathology of Crinivirus infections
812 in different plant hosts. Ann Appl Biol 143:99–110. <https://doi.org/10.1111/j.1744-7348.2003.tb00274.x>
- 814 Milenovic M, Wosula EN, Rapisarda C, Legg JP (2019) Impact of host plant species and
815 whitefly species on feeding behavior of *Bemisia tabaci*. Front Plant Sci 10:1.
816 <https://doi.org/10.3389/fpls.2019.00001>
- 817 Mitchell C, Brennan RM, Graham J, Karley AJ (2016) Plant defense against herbivorous
818 pests: exploiting resistance and tolerance traits for sustainable crop protection. Front

- 819 Plant Sci 7:1132. <https://doi.org/10.3389/fpls.2016.01132>
- 820 Mugford ST, Barclay E, Drurey C, et al (2016) An immuno-suppressive aphid saliva protein
821 is delivered into the cytosol of plant mesophyll cells during feeding. *Mol Plant Microbe*
822 *Interact* 29:854–861. <https://doi.org/10.1094/MPMI-08-16-0168-R>
- 823 Nachappa P, Margolies DC, Nechols JR, et al (2013) Tomato spotted wilt virus benefits a
824 non-vector arthropod, *Tetranychus Urticae*, by modulating different plant responses in
825 tomato. *PLoS One* 8:1–14. <https://doi.org/10.1371/journal.pone.0075909>
- 826 Ng JC, Zhou JS (2015) Insect vector–plant virus interactions associated with non-circulative,
827 semi-persistent transmission: current perspectives and future challenges. *Curr Opin*
828 *Virol* 15:48–55. <https://doi.org/10.1016/j.coviro.2015.07.006>
- 829 Núñez-Farfán J, Fornoni J, Valverde PL (2007) The evolution of resistance and tolerance to
830 herbivores. *Annu Rev Ecol Evol Syst* 38:541–566.
831 <https://doi.org/10.1146/annurev.ecolsys.38.091206.095822>
- 832 Peñafior MFGV, Mauck KE, Alves KJ, et al (2016) Effects of single and mixed infections of
833 Bean pod mottle virus and Soybean mosaic virus on host-plant chemistry and host-
834 vector interactions. *Funct Ecol* 30:1648–1659. <https://doi.org/10.1111/1365-2435.12649>
- 835 Pereira LS, Lourenção AL, Salas FJS, et al (2019) Infection by the semi-persistently
836 transmitted Tomato chlorosis virus alters the biology and behaviour of *Bemisia tabaci* on
837 two potato clones. *Bull Entomol Res* 1–8. <https://doi.org/10.1017/S0007485318000974>
- 838 Peng H-C, Walker GP (2018) Sieve element occlusion provides resistance against *Aphis*
839 *gossypii* in TGR-1551 melons. *Insect Sci*. <https://doi.org/10.1111/1744-7917.12610>
- 840 Rajabaskar D, Wu Y, Bosque-Pérez NA, Eigenbrode SD (2013) Dynamics of *Myzus*
841 *persicae* arrestment by volatiles from Potato leafroll virus-infected potato plants during
842 disease progression. *Entomol Exp Appl* 148:172–181
- 843 Rodriguez PA, Stam R, Warbroek T, Bos JIB (2014) Mp10 and Mp42 from the aphid species
844 *Myzus persicae* trigger plant defenses in *Nicotiana benthamiana* through different
845 activities. *Mol Plant Microbe Interact* 27:30–39. <https://doi.org/10.1094/MPMI-05-13-0156-R>
- 847 Roosien BK, Gomulkiewicz R, Ingwell LL, et al (2013) Conditional vector preference aids the
848 spread of plant pathogens: results from a model. *Environ Entomol* 42:1299–1308.
849 <https://doi.org/10.1603/EN13062>
- 850 Salvaudon L, De Moraes CM, Mescher MC (2013) Outcomes of co-infection by two
851 potyviruses: implications for the evolution of manipulative strategies. *Proc Biol Sci*
852 280:20122959. <https://doi.org/10.1098/rspb.2012.2959>
- 853 Shaw AK, Peace A, Power AG, Bosque-Pérez NA (2017) Vector population growth and
854 condition-dependent movement drive the spread of plant pathogens. *Ecology* 98:2145–
855 2157. <https://doi.org/10.1002/ecy.1907>
- 856 Shrestha D, McAuslane HJ, Ebert TA, et al (2019) Assessing the temporal effects of Squash
857 vein yellowing virus infection on settling and feeding behavior of *Bemisia tabaci*
858 (MEAM1) (Hemiptera: Aleyrodidae). *J Insect Sci* 19.:
859 <https://doi.org/10.1093/jisesa/iez036>
- 860 Stukenberg N, Poehling H (2019) Blue–green opponency and trichromatic vision in the

- 861 greenhouse whitefly (*Trialeurodes vaporariorum*) explored using light emitting diodes.
862 Ann Appl Biol 175:146–163. <https://doi.org/10.1111/aab.12524>
- 863 Su Q, Mescher MC, Wang S, et al (2016) Tomato yellow leaf curl virus differentially
864 influences plant defence responses to a vector and a non-vector herbivore. Plant Cell
865 Environ 39:597–607. <https://doi.org/10.1111/pce.12650>
- 866 Tjallingii WF (1988) Electrical recording of stylet penetration activities. In: Aphids: Their
867 Biology, Natural Enemies and Control. World Crop Pests., Elsevier. Amsterdam, The
868 Netherlands, pp 95–108
- 869 Tjallingii WF, Hogen Esch T (1993) Fine structure of aphid stylet routes in plant tissues in
870 correlation with EPG signals. Physiol Entomol 18:317–328.
871 <https://doi.org/10.1111/j.1365-3032.1993.tb00604.x>
- 872 Tzanetakis IE, Martin RR, Wintermantel WM (2013) Epidemiology of criniviruses: an
873 emerging problem in world agriculture. Front Microbiol 4:119.
874 <https://doi.org/10.3389/fmicb.2013.00119>
- 875 Werner BJ, Mowry TM, Bosque-Pérez NA, et al (2009) Changes in green peach aphid
876 responses to Potato leafroll virus–induced volatiles emitted during disease progression.
877 Environ Entomol 38:1429–1438. <https://doi.org/10.1603/022.038.0511>
- 878 Wintermantel WM, Gilbertson RL, Natwick ET, et al (2009) Epidemiology of Cucurbit yellow
879 stunting disorder virus in California is influenced by an expanded host range of non-
880 cucurbit weed and crop species. Phytopathology 99:S142
- 881 Wintermantel WM, Gilbertson RL, Natwick ET, McCreight JD (2017) Emergence and
882 epidemiology of Cucurbit yellow stunting disorder virus in the American Desert
883 Southwest, and development of host plant resistance in melon. Virus Res 241:213–219.
884 <https://doi.org/10.1016/j.virusres.2017.06.004>
- 885 Wintermantel WM, Wisler GC (2006) Vector specificity, host range, and genetic diversity of
886 Tomato chlorosis virus. Plant Dis 90:814–819. <https://doi.org/10.1094/PD-90-0814>
- 887 Wood SN (2017) Generalized additive models: an introduction with R. Chapman and
888 Hall/CRC
- 889 Xu H-X, Qian L-X, Wang X-W, et al (2019) A salivary effector enables whitefly to feed on
890 host plants by eliciting salicylic acid-signaling pathway. Proc Natl Acad Sci U S A
891 116:490–495. <https://doi.org/10.1073/pnas.1714990116>
- 892 Zarate SI, Kempema LA, Walling LL (2007) Silverleaf whitefly induces salicylic acid defenses
893 and suppresses effectual jasmonic acid defenses. Plant Physiol 143:866–875.
894 <https://doi.org/10.1104/pp.106.090035>
- 895 Ziegler-Graff V (2020) Molecular insights into host and vector manipulation by plant viruses.
896 Viruses 12.: <https://doi.org/10.3390/v12030263>

897

898 **Figure captions**

899 **Figure 1.** Whitefly behavioral responses to contact, volatile and visual cues of sham-
900 inoculated (i.e., non-infected) and CYSDV-infected melon plants after 1h, 2h and 24h. Thirty

901 whiteflies were allowed to settle on melon leaves of two non-infected and two infected plants
 902 either two- or four- weeks post-inoculation. Twenty-four replicates were performed (N=24).
 903 Letters indicate significant differences associated with Friedman tests followed by pairwise
 904 comparisons using Wilcoxon signed rank tests.

905 **Figure 2.** Effect of 4 wpi CYSDV-infected melon leaves symptoms (yellow discoloration) on
 906 whitefly settlement preferences (data from tests in Fig. 1) (a) and response of whiteflies to
 907 volatile cues from 4 wpi plants in contact and visual-cue free choice tests (N=16) (b).

908 **Figure 3.** Aphid behavioral responses to contact, volatile and visual cues of sham-inoculated
 909 (i.e., non-infected) and CYSDV-infected melon plants after 1h, 2h and 24h. Twenty aphids
 910 were allowed to choose between a leaf from each of one non-infected and one infected plant
 911 either (a) two weeks post-inoculation or (b) four weeks post-inoculation. Between twenty and
 912 twenty-two replicates were performed for each modality. Asterisks indicate significant
 913 differences (** $P < 0.01$, NS: not significant) as determined using Wilcoxon tests.

914 **Figure 4.** Durations of pathway phases, phloem salivation phase, and phloem sap ingestion
 915 phase of (a) *Bemisia tabaci* and (b) *Aphis gossypii* on CYSDV-infected or sham-inoculated
 916 melon plants after two- or four-weeks post-inoculation (wpi) (N=20-24).

917 **Figure 5.** Effect of CYSDV-infection after (a) two weeks post-inoculation (wpi) or (b) four
 918 weeks post-inoculation (wpi) on whitefly fecundity. Data shown are the means +/- standard
 919 errors of the means of data from 22 to 32 repetitions. Asterisks indicate significant
 920 differences between CYSDV-infected plants and sham-inoculated plants (EMMeans pairwise
 921 comparisons, * $P < 0.05$, ** $P < 0.01$).

922 **Figure 6.** Effect of CYSDV infection on *Aphis gossypii* population size. Aphids were allowed
 923 to reproduce on plants between 18 dpi and 29 dpi (transition from pre-symptomatic 2 wpi to
 924 symptomatic 4 wpi period). Data shown are mean +/- standard errors for two temporally
 925 separated repetitions of the experiment (batch 1 and batch 2), each with 6-8 replicate plants
 926 in each treatment. Letters indicate significant differences between CYSDV-infected plants
 927 and Sham-inoculated plants (EMMeans pairwise comparisons, $P < 0.05$).

928 **Figure 7.** Quantifications of sucrose, glucose, and fructose in leaf tissue samples taken from
 929 upper leaves (asymptomatic across time points) (a, b and c) and the lower leaves (same as
 930 those used in all bioassays for each disease progression time point) (d, e, f). Data displayed
 931 as means +/- standard errors with 8 replicate plants in each treatment x disease progression
 932 x leaf position combination. Analyses on upper and lower leaves were performed separately,
 933 with post-hoc Tukey tests when significant main effects were detected. Letters within each

934 graph indicate significant differences at $P < 0.05$.

935 **Figure 8.** Constrained PCA score plots of multivariate analyses (RDA) for amino acids only,
936 illustrating interactions of infection status with time point (a), infection status with leaf position
937 (b) and leaf position with time point (c). CY and SH designate CYSDV-infected and sham-
938 inoculated, respectively, in both plots. In graphs (a) and (b) these treatments also maintain
939 the green (SH) and yellow (CY) color codes used throughout the other figures. Graph (c)
940 pools data across the SH and CY treatments. In this graph U (in red) and L (in blue) refer to
941 upper and lower leaf samples and 2wk and 4wk refer to stages of disease progression (2 wpi
942 and 4wpi).

943 **Figure 9.** Volatile blend analyses illustrating effects of CYSDV infection (4 wpi) on blend
944 composition. Plot (a) is a score plot from a multivariate analysis (PPLS-DA) with infection
945 status as the factor (analysis details in ESM). Plot (b) shows sample clustering for the
946 random forest analysis (decision-tree based method, analysis details in ESM). Means \pm SE
947 for individual volatile components of each blend are included in Table S5 in ESM).

948 **Table 1:** GC-MS operating parameters and non-volatile metabolite quantification

GC-MS Parameter	Details
Sample volume	1 μ L
Inlet temperature; mode	230°C; splitless mode
Carrier gas; inlet flow rate	Helium (99.9999% UHP200); 1 ml/min constant
Split flow rate; splitless time	25 mL/min; 0.8 min
Purge flow rate; septum purge	5 mL/min; constant
Gas saver	Enabled at 25 mL/min, initiated at 2 min
Column	Thermo Scientific TG-5MS (0.25 mm i.d. x 28.33 m, 0.25 μ m film thickness)
Temperature program	70 °C for 5 min, followed by a 5 °C/min ramp to 325 °C, and a hold at this temperature for 1 min (total time 57 min)
Transfer line/MS source temps	250 °C/230 °C
MS mode	Single quadrupole, electron ionization, general acquisition (scan) mode starting at 5.95 minutes
Mass range for scanning	50-600
Dwell time	0.2s
Quality control for identifications and major ion selection	Commercial standards for each metabolite
Quantification	Individual channels for each compound were extracted from Total Ion Chromatogram (TIC) by specifying the mass range for the major ion detected in each standard
Standardization	Individual metabolite amount (μ g/g tissue) = Total peak areas (counts*min) of each compound / peak area of internal standard (ribitol) * 12 (12 μ g ribitol spiked in each sample) / tissue weight (g)

949

950 **Table 2:** GC-MS operating parameters and volatile metabolite quantification

GC-MS Parameter	Details
Sample volume	1 μ L
Inlet temperature; mode	280°C; splitless mode
Carrier gas; inlet flow rate	Helium (99.9999% UHP200); 3ml/min constant
Split flow rate; splitless time	24mL/min; 0.8min
Purge flow rate; septum purge; vacuum compensation	5mL/min; constant; constant
Gas saver	Enabled at 25mL/min, initiated at 2 min
Column	Thermo Scientific TG-5MS (0.25 mm i.d. \times 28.33 m, 0.25 μ m film thickness)
Temperature program	40°C for 1 min, ramp to 100°C at a rate of 4°C/min, ramp to 280°C at a rate of 8°C/min, hold at 280°C for 1 min
Transfer line/MS source temps	280°C/250°C
MS mode	Single quadrupole, electron ionization, general acquisition (scan) mode starting at 2.95 minutes
Mass range for scanning	50-600
Dwell time	0.2s
Identifications	NIST 2014 library and commercial standards for each metabolite if available
Quantification	Peak areas in resulting chromatograms were integrated to calculate area using Chromeleon software
Standardization	Individual metabolite amount (ng/g tissue) = Total peak areas (counts*min) of each compound / peak area of internal standard (nonyl acetate) * 600 (600ng ribitol spiked in each sample) / tissue weight (g)

951

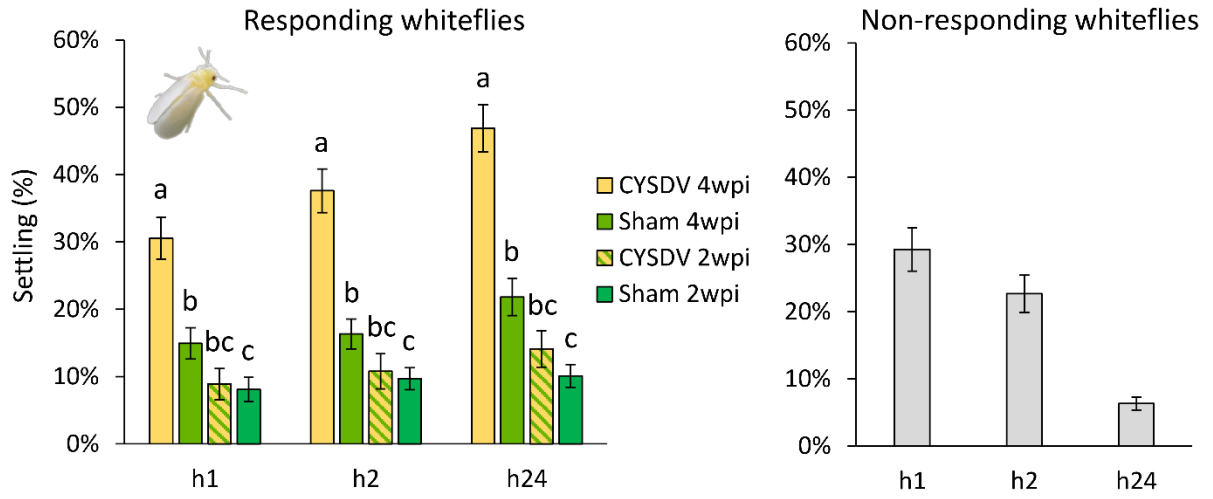
952

953 **Table 3:** Permutation F-tests of the factors included in Redundancy Analysis (RDA) (999
954 permutations) to identify main drivers of variation in leaf metabolite composition (compound
955 identity and quantity).

	<i>F</i>	<i>P</i>
Infection status	0.464	0.906
Time point	9.491	0.001 ***
Leaf position	5.810	0.001 ***
Infection x Time	3.084	0.004 **
Infection x Leaf	2.431	0.017 *
Time x Leaf	3.572	0.003 **
Infection x Time x Leaf	1.117	0.294

956 Significant P-values are indicated in bold (* P < 0.05; ** P < 0.01; *** P < 0.001). Pairwise
957 comparisons are available in the ESM (Table S1).

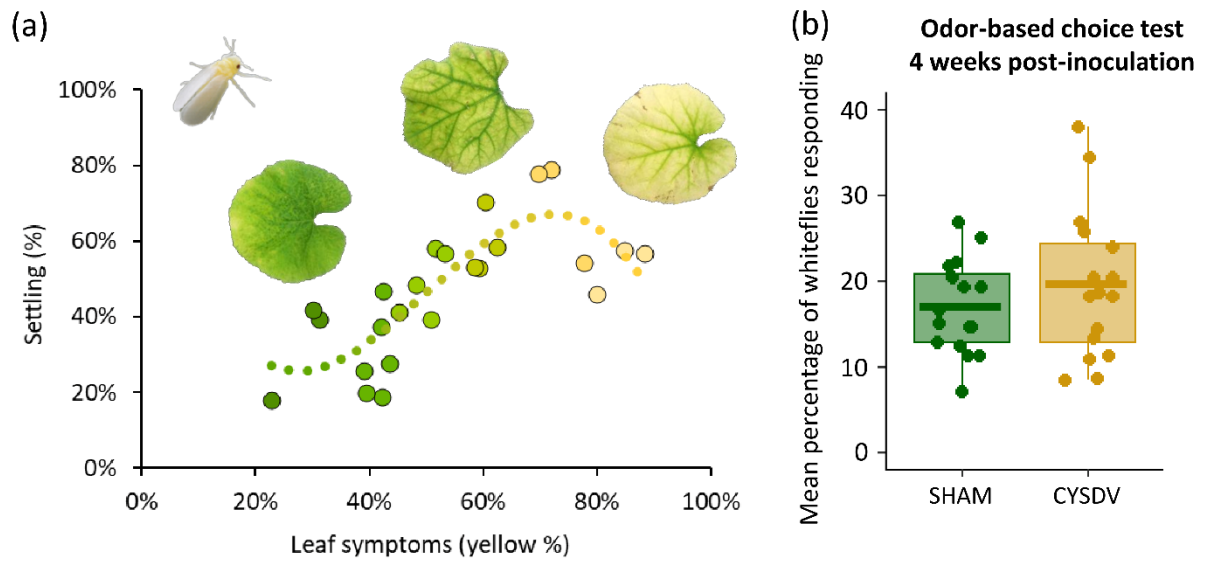
958



959

960 **Figure 1.**

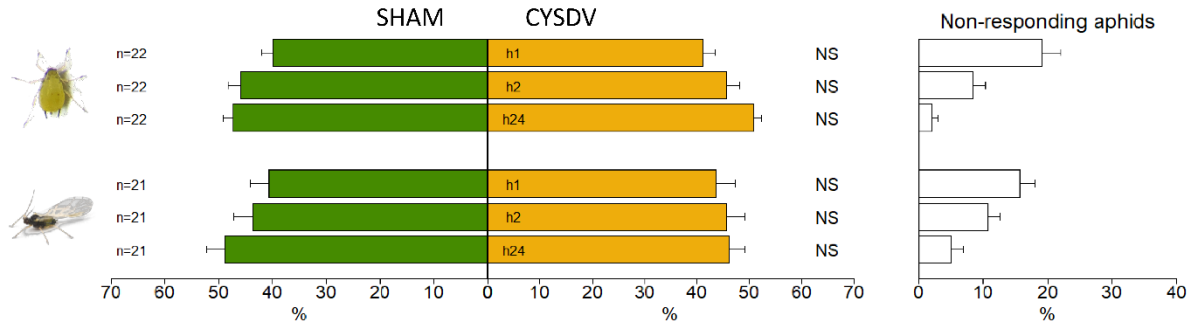
961



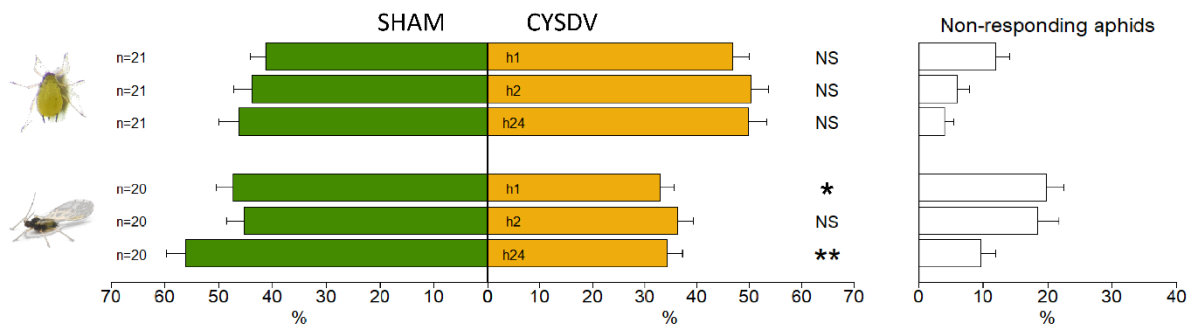
962

963 **Figure 2.**

(a) Two weeks post-inoculation

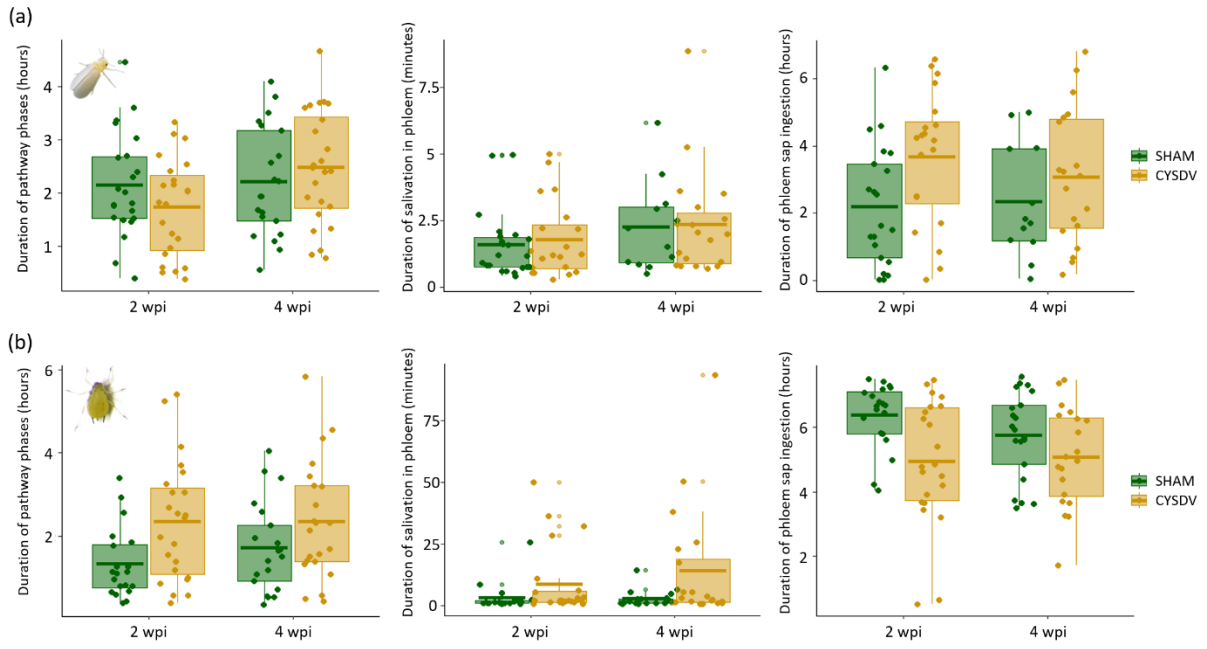


(b) Four weeks post-inoculation



964

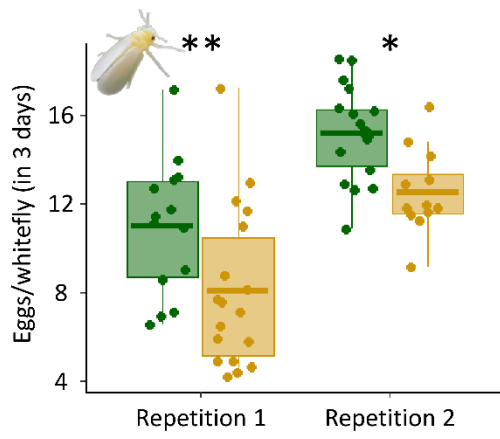
965 **Figure 3.**



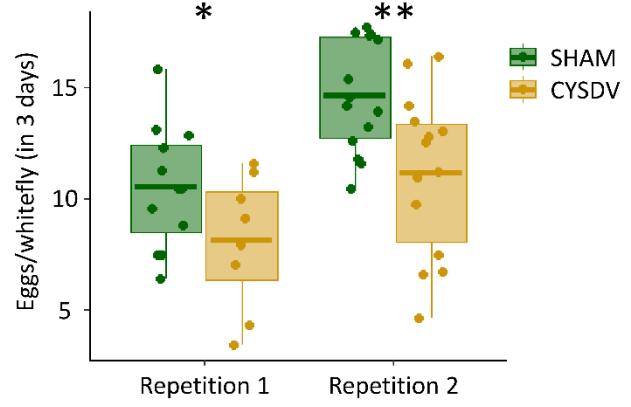
966

967 **Figure 4.**

(a) Two weeks post-inoculation

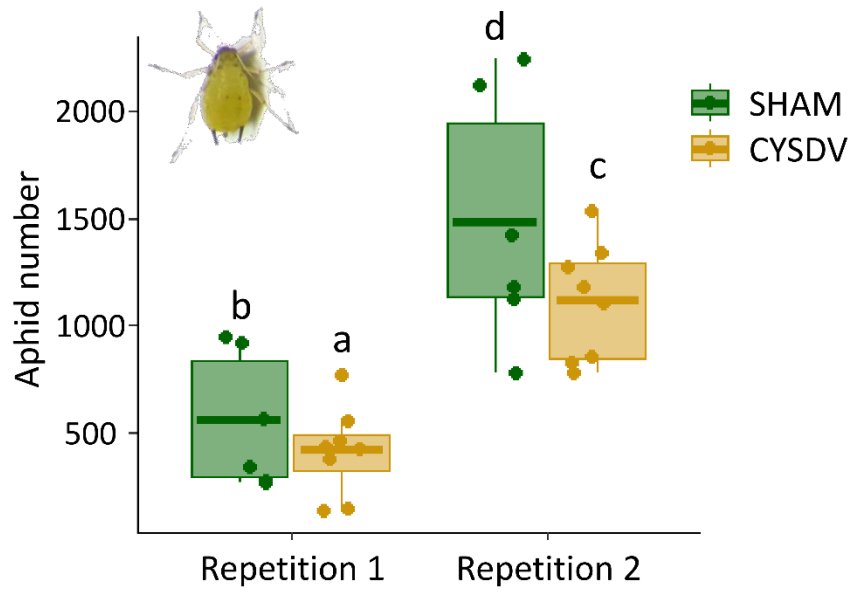


(b) Four weeks post-inoculation



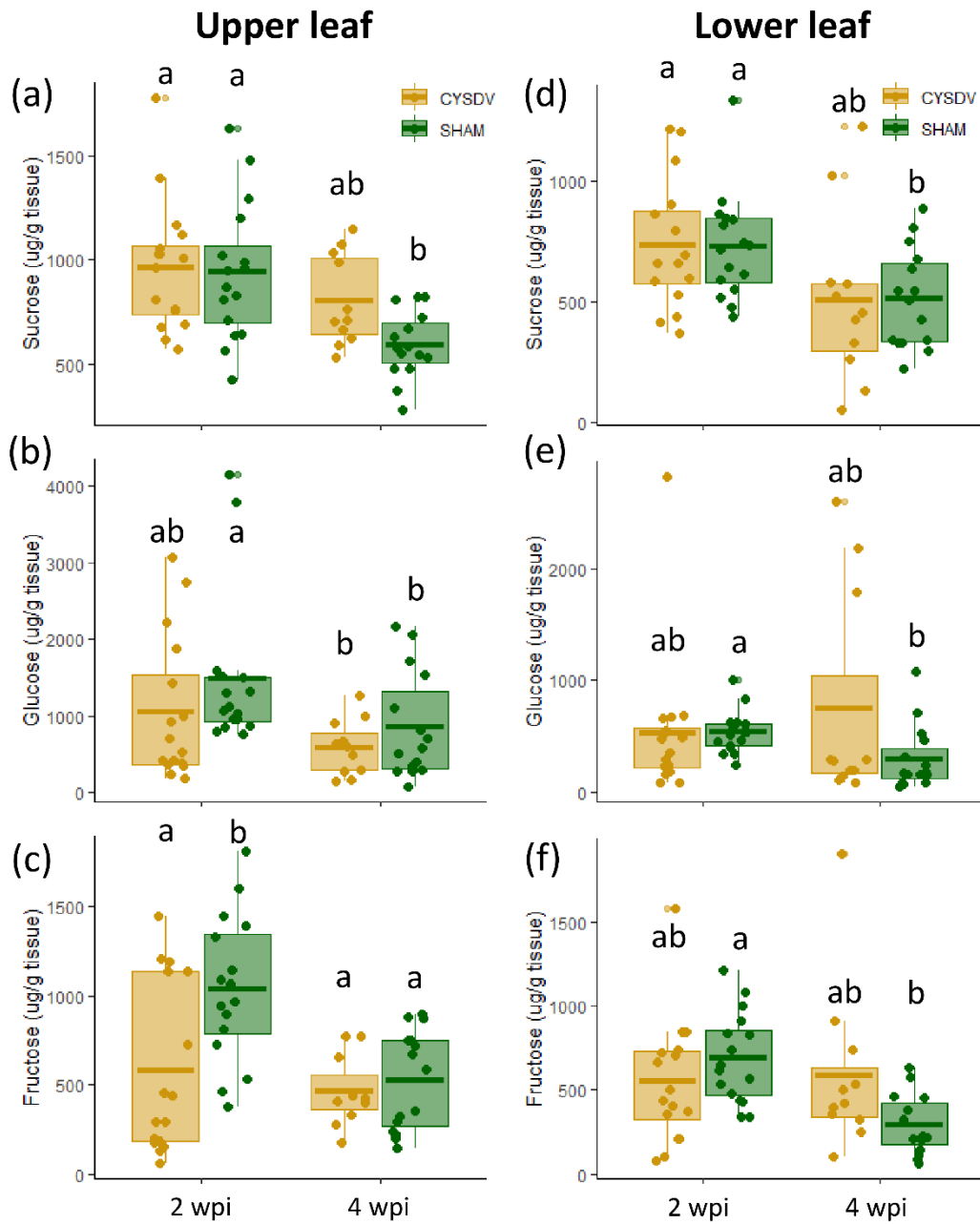
968

969 **Figure 5.**



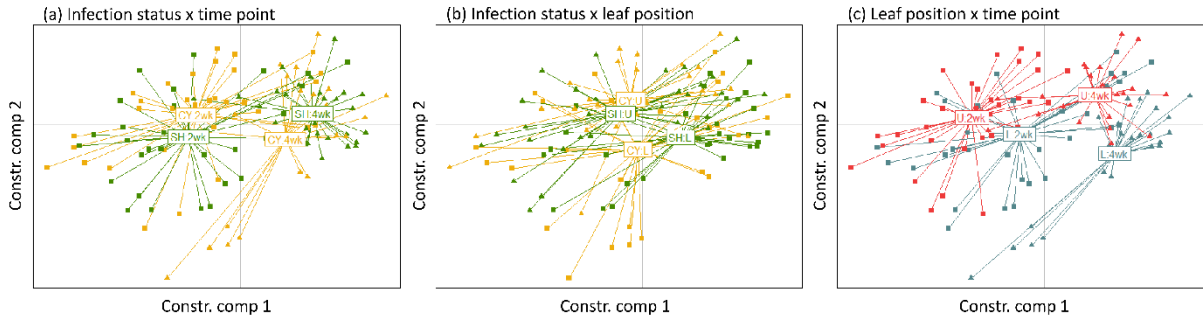
970

971 **Figure 6.**



972

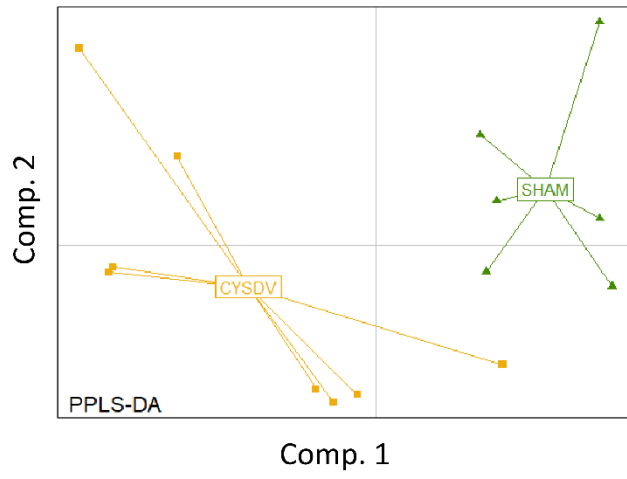
973 **Figure 7.**



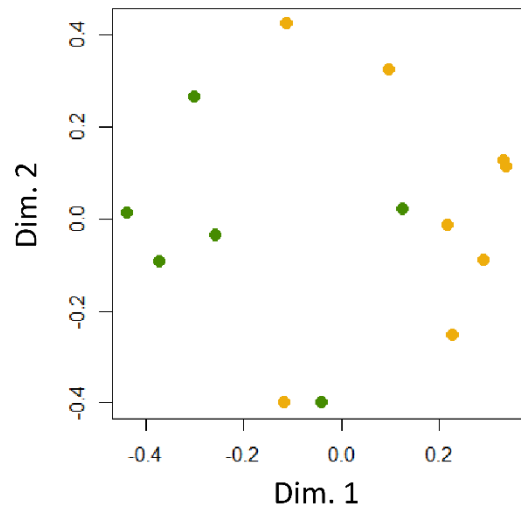
974

975 **Figure 8.**

(a) PPLS-DA



(b) Random Forest



976

977 **Figure 9.**